# Highly Permeable Reverse Osmosis Membranes via Molecular Layer-by-Layer Deposition of Trimesoyl Chloride and 3,5-Diaminobenzoic Acid

William D. Mulhearn and Christopher M. Stafford*

*Corresponding author E-mail: chris.stafford@nist.gov

Materials Science and Engineering Division, National Institute of Standards and Technology, Gaithersburg, MD 20899, USA

**ABSTRACT**

We present a series of polyamide membranes synthesized via molecular layer-by-layer (mLbL) deposition of trimesoyl chloride (TMC) and 3,5-diaminobenzoic acid (BA). These membranes exhibit superior NaCl rejection compared to previously reported TMC-BA membranes prepared via interfacial polymerization, with the improved performance of the mLbL films attributable to higher cross-link density facilitated by the stepwise deposition process in good solvents. We compare the TMC-BA series with membranes synthesized from TMC and *m*-phenylenediamine (MPD), a conventional reverse osmosis membrane chemistry. At the minimum thickness capable of 90 % NaCl rejection, mLbL TMC-BA membranes exhibit 50 % greater water permeance than mLbL TMC-MPD.

**Keywords:** Polyamide, membranes, desalination, molecular layer-by-layer deposition, solution-diffusion, permeance

**TOC Graphic**

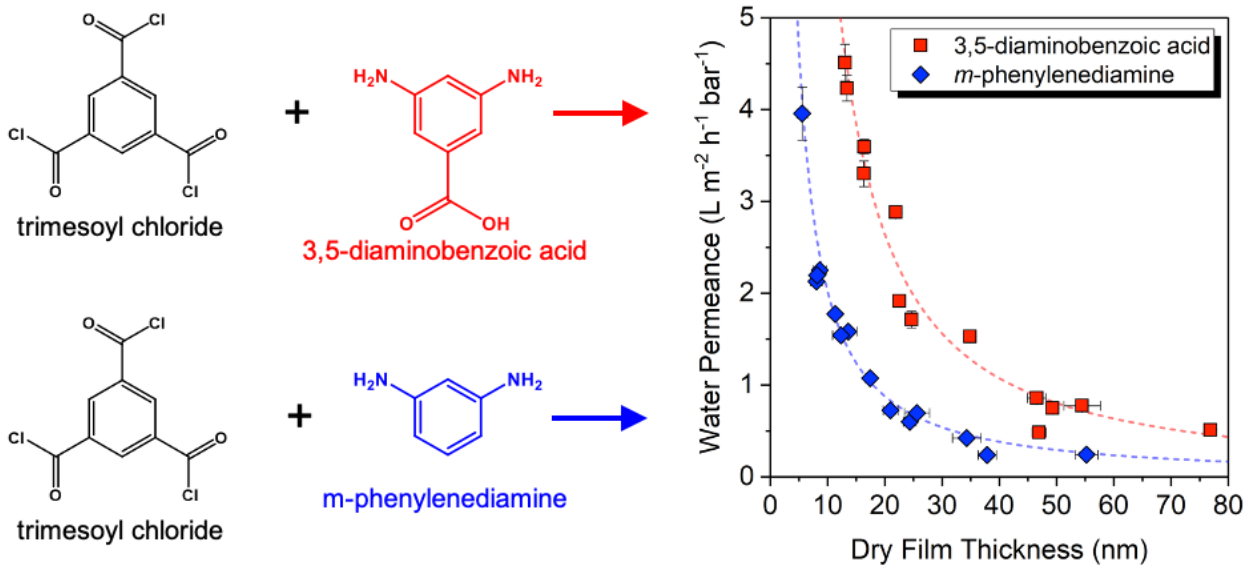
trimesoyl chloride
3,5-diaminobenzoic acid
trimesoyl chloride
m-phenylenediamine
3,5-diaminobenzoic acid
m-phenylenediamine
Water Permeance (L m-2 h-1 bar-1)
Dry Film Thickness (nm)

## Introduction

Commercial reverse osmosis (RO) membranes for water desalination are conventionally prepared by interfacial polymerization (IP) of a triacid chloride and a diamine, atop a macroporous support layer.[1–3] The properties of the resulting polyamide (PA) selective layer depend strongly on the chemistry of the monomers[2,4–6] and the details of the synthesis method.[4,5,7] Variations in monomer chemistry and reaction conditions have large implications for the network cross-link density, the type and concentration of polar functional groups at the membrane surface and in the interior, and void size or free volume within the membrane that facilitates transport.

The common PA chemistry for RO membranes targeting the removal of monovalent ions consists of trimesoyl chloride (TMC) and *m*-phenylyenediamine (MPD). Still, there remains active interest in developing new monomer chemistries that may offer superior performance. According to the solution-diffusion model, the water permeance, $A$, of a membrane is proportional to the thermodynamic sorption coefficient $K_{w,m}$, a measure of the membrane's capacity to swell in water at equilibrium. Permeance is defined as the water flux, $J_w$, normalized by the difference between the applied and osmotic pressures, $\Delta P - \Delta\pi$, and is described by the solution-diffusion model[2,8] according to,

$$A \equiv \frac{J_w}{\Delta P - \Delta\pi} = \frac{D_{w,m} K_{w,m} c_{w,f} v_w}{h_m R T} \quad (1)$$

where $D_{w,m}$ is the diffusion coefficient of water in the membrane, $c_{w,f}$ is the molar concentration of water in the feed, $v_w$ is the molar volume of water, $h_m$ is the membrane thickness, $R$ is the gas constant, and $T$ is the absolute temperature. As such, increasing $K_{w,m}$ by controlling the hydrophilicity of the PA layer may improve solution permeance.[9–15] One candidate chemistry replaces MPD with 3,5-diaminobenzoic acid (BA); structural similarity between the two

diamines may promote similar reactivity and therefore similar cross-link density, while substantially improving hydrophilicity via the pendant carboxylic acid. The chemical structures of the monomers and the TMC-MPD and TMC-BA polymers are illustrated in Figure 1. In TMC-MPD, the carboxylic acid content is entirely associated with incomplete cross-linking and is therefore very low for highly cross-linked RO membranes.

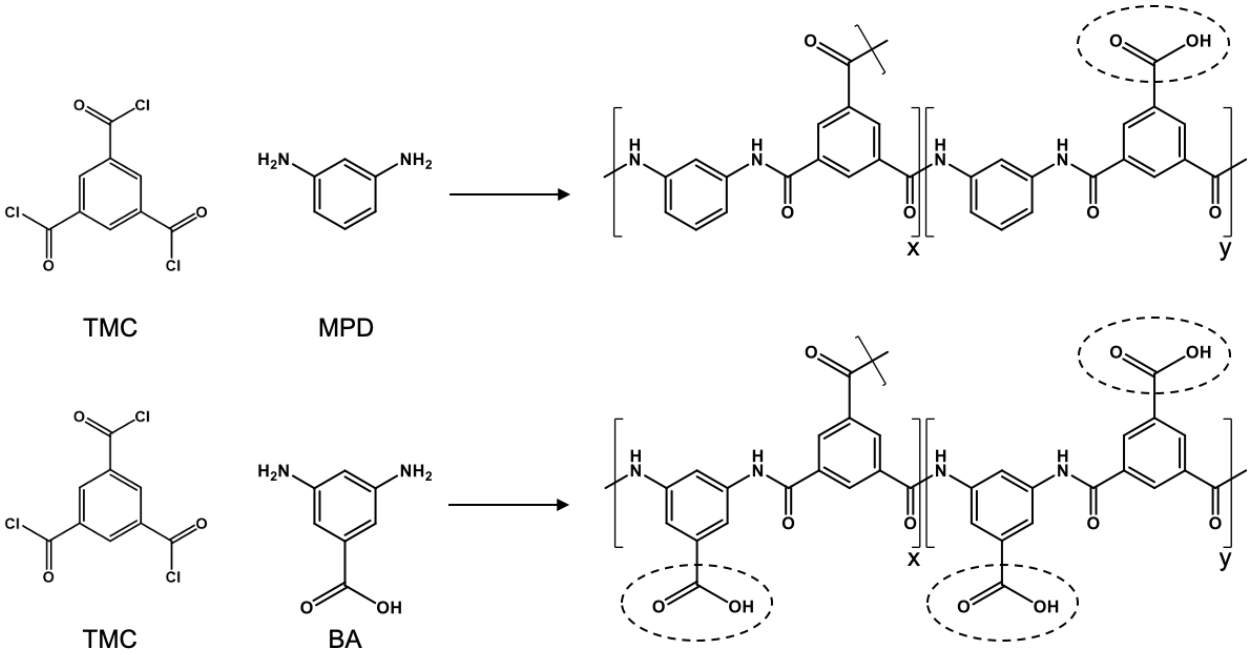


**Figure 1.** Chemical structures of TMC, MPD, and BA, and the polyamides from their respective polymerization and subsequent conversion of unreacted acid chloride into carboxylic acid via exposure to water. Subscripts *x* and *y* refer to the fractions of fully reacted and partially reacted TMC in the network, respectively, such that $x = 1$ and $y = 0$ for a completely cross-linked network. Polar carboxylic acid groups are circled for emphasis.

Several attempts have been reported to synthesize IP membranes from TMC and BA, however these studies have generally shown poor rejection of monovalent salts. Roh and

colleagues reported an IP TMC-BA membrane exhibiting 24 % NaCl rejection, albeit with good water permeance of 2.3 L $m^{-2}$ $h^{-1}$ $bar^{-1}$, compared to IP TMC-MPD with 98 % NaCl rejection and water permeance of 0.25 L $m^{-2}$ $h^{-1}$ $bar^{-1}$ in the same study.[9] Saha and Joshi later reported an improved IP TMC-BA membrane exhibiting 67 % NaCl rejection and water permeance of 5.6 L $m^{-2}$ $h^{-1}$ $bar^{-1}$,[10] although this salt rejection still falls short of a high-performance RO membrane. Other studies incorporated BA, but either with a different acid chloride or with the addition of a third reactive species such that BA was a small minority component of the resulting polymer. Gupta prepared linear polymers from isophthaloyl chloride (IPC) and BA as well as terephthaloyl chloride (TPC) and BA, which were cast into thick membranes reported to exhibit between 80 % and 98 % NaCl rejection with water permeance between 0.45 L $m^{-2}$ $h^{-1}$ $bar^{-1}$ and 0.95 L $m^{-2}$ $h^{-1}$ $bar^{-1}$.[11] However, Gupta's result is an outlier for this chemistry, with three more recent studies of the same material indicating different performance. Aiba and colleagues also synthesized linear IPC-BA polyamide, which was cast into membranes with 23 % NaCl rejection and water permeance of 0.12 L $m^{-2}$ $h^{-1}$ $bar^{-1}$.[12] Roh and colleagues prepared IP membranes from IPC-BA and TPC-BA with 17 % and 7 % NaCl rejection, respectively, and water permeance of 2.7 L $m^{-2}$ $h^{-1}$ $bar^{-1}$ and 3.0 L $m^{-2}$ $h^{-1}$ $bar^{-1}$, respectively.[9] Saha and Joshi likewise prepared IP membranes from IPC-BA with 23 % NaCl rejection and water permeance of 13 L $m^{-2}$ $h^{-1}$ $bar^{-1}$.[10] It is therefore reasonable to conclude that linear BA-containing PA lacks the tight network structure needed to restrict the passage of hydrated salt ions, presumably due to the high degree of swelling in these films without cross-links to resist network expansion.

The earliest report of a cross-linked three-component film containing BA is a patent by Kim and colleagues, in which IP of an aqueous solution of 2 parts by mass of 4,4′-dihydroxybiphenyl to 1 part by mass of BA, with a solution of TMC in *n*-hexane yields a

membrane exhibiting 94 % NaCl rejection and water permeance of 2.1 L $m^{-2}$ $h^{-1}$ $bar^{-1}$.[16] However, the proportion of BA incorporated into the polymer was not quantified. Owing to the very poor solubility of BA in the *n*-hexane organic phase to access the polymerization site, located within the organic phase close to the interface,[17–22] it is likely that this proportion is extremely small, as elaborated below. Following Kim's three-component approach, a series of studies by Ahmad and colleagues[13–15] reported membranes prepared via IP of TMC in the organic phase with a mixture of piperazine (PIP) and BA in the aqueous phase. The solution flux and salt rejection of these membranes strongly depended on the ratio of PIP to BA. NaCl rejection spanned 12 % to 62 %, and water permeance spanned 3.2 L $m^{-2}$ $h^{-1}$ $bar^{-1}$ to 12 L $m^{-2}$ $h^{-1}$ $bar^{-1}$, where raising the BA proportion in the reaction mixture monotonically decreased the salt rejection and either monotonically increased the water permeance[13] or reached a local maximum in water permeance at intermediate BA content.[15]

**Results and Discussion**

Based on this survey, no pure TMC-BA membranes with consistently high NaCl rejection have been prepared to date. Poor salt rejection is likely attributable to loose network structure, a result either of the steric bulk of the BA or the poor solubility of BA in the nonpolar organic solvents used for IP. In this work, we present TMC-BA membranes prepared via molecular layer-by-layer (mLbL) assembly[23,24]. We utilize an mLbL synthesis method because the resulting membranes are expected to exhibit higher cross-link densities than IP membranes, as the reactive species are not required to diffuse across the as-forming polyamide at the interface to find available reactive sites, and mLbL films have been shown to exhibit very low surface roughness relative to IP[23] that enables accurate and unambiguous characterization of the active layer thickness. Furthermore, IP requires that the diamine monomer partition from the

aqueous phase into the organic phase, typically hexanes or Isopar, to reach and react with the forming polymer. However, the solubility of many diamines in organic solvents is quite low. Specifically, the measured solubilities of BA in various solvents are listed in Table 1.

| Solvent | BA Solubility (mg/mL) |
|---|---|
| Tetrahydrofuran | 16.15 |
| Water | 8.65 |
| Isopropanol | 1.43 |
| Toluene | 0.06 |
| Hexanes | 0.00 |

**Table 1.** Solubility of BA in selected solvents at 23 °C. In all cases, the measurement uncertainty is ±0.01 mg/mL.

We detect no solubility of BA in hexanes, suggesting that many of the IP membranes described above likely contain little BA or have low cross-link densities owing to very poor access of BA to the polymerization site. In contrast, mLbL synthesis allows us to select solvents well suited to the monomers. In our study here, TMC deposition and rinse steps are performed using toluene, as reported for the conventional mLbL deposition process, while BA deposition and rinse steps are performed using tetrahydrofuran to facilitate availability of BA monomer to the forming mLbL film and subsequent removal of any unreacted monomer.

While some prior studies primed the support layer with a polyelectrolyte barrier layer before synthesizing the mLbL active layer directly atop a macroporous support,[25,26] we instead synthesize our membranes on silicon wafers coated with a water-soluble poly(sodium 4-styrene sulfonate) (PSS) release layer and subsequently transfer to a polyacrylonitrile (PAN) layer for

performance testing. We chose this two-step approach since it has not been definitively shown that the barrier layer does not participate in the reaction. Furthermore, by eliminating the barrier layer we can reliably measure the active layer thickness and provide absolute measurements of the active layer permeance.

Desalination performance testing was carried out on each of the TMC-BA and TMC-MPD membranes by challenging with ≈1000 mg/L NaCl aqueous solutions in a stirred dead-end filtration cell at an applied pressure of $\Delta P$ = 34.5 bar (500 psi, or 3.45 MPa). The measured water flux is divided by the difference between the applied pressure and the osmotic pressure across the membrane at the time of collection, $\Delta\pi$ = (0.80 to 0.95) bar, to give the water permeance. The solute rejection is defined as,

$$R = \left(1 - \frac{c_p}{c_f}\right) \times 100\ \% \qquad (2)$$

where $c_f$ and $c_p$ are the NaCl concentrations of the feed and of the permeate, respectively. The feed NaCl concentration and osmotic pressure are recalculated at each time of collection, based on the total volumes and concentrations of the collected permeate solution. The results of the desalination performance tests are shown in Figure 2. For comparison, a control measurement on a DuPont pilot-scale brackish water membrane in the same dead-end apparatus at $\Delta P$ = 34.5 bar displayed a water permeance of 3.6 L $m^{-2}$ $h^{-1}$ $bar^{-1}$ with NaCl rejection of 97.5 %, and a bare macroporous PAN layer had a water permeance of 620 L $m^{-2}$ $h^{-1}$ $bar^{-1}$ measured at $\Delta P$ = 6.9 bar.

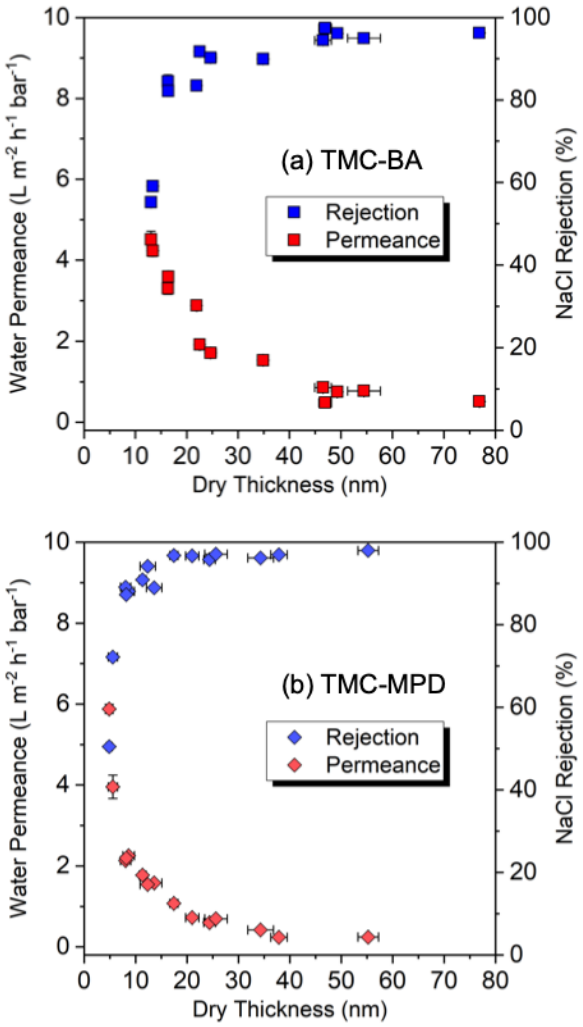


**Figure 2.** Water permeance and NaCl rejection vs. PA membrane thickness for (a) TMC-BA and (b) TMC-MPD. Applied pressure $\Delta P$ = 34.5 bar, and initial feed concentration $c_{f,0} \approx$ 1000 mg/L NaCl. The error bars represent one standard deviation of the data ($n$ = 3 to 5), which is taken as the experimental uncertainty of the measurement. Some error bars are smaller than the symbols.

The water permeance and NaCl rejection curves are qualitatively similar between the TMC-BA series and the TMC-MPD series. In both cases, water permeance smoothly decreases with film thickness, and NaCl rejection increases rapidly at low film thickness before stabilizing above a critical thickness. Plots of water permeance vs. reciprocal dry thickness are provided in

the Supporting Information for both membrane chemistries. Both TMC-BA and TMC-MPD exhibit deviations from the solution-diffusion model prediction, permeance $\propto 1 / h$, for the thinnest films in both sets, suggesting that the mLbL polyamide material properties evolve as the film grows, stabilizing at intermediate film thicknesses of (10 to 20) nm.

Two quantitative differences between the data sets are that the water permeance of TMC-BA is approximately 2.5 times that of TMC-MPD with the same dry thickness, and the turnover to a high NaCl rejection of 90 % occurs at a larger thickness for TMC-BA (roughly 20 nm to 30 nm) compared to TMC-MPD (roughly 10 nm to 15 nm). Selecting 90 % NaCl rejection as a performance benchmark, the optimal TMC-MPD film thickness is about 15 nm, corresponding to water permeance slightly greater than 1.5 L $m^{-2}$ $h^{-1}$ $bar^{-1}$. In comparison, for that same performance benchmark the optimal TMC-BA film thickness is about 25 nm, corresponding to water permeance of slightly greater than 2.2 L $m^{-2}$ $h^{-1}$ $bar^{-1}$. Thus, the TMC-BA chemistry offers a 47 % increase in permeance relative to TMC-MPD when both films are prepared at a thickness consistent with the benchmark performance.

The enhanced transport of TMC-BA membranes is associated with an increase in the hydrophilicity of the membrane, as indicated by a decrease in the static water contact angle from 67° ± 2° for TMC-MPD to 43° ± 2° for TMC-BA, in addition to the swelling ratio in water. The equilibrium swelling ratios of TMC-BA membranes are shown in Figure 3 for a range of dry film thicknesses. In each case, the swelling ratio is calculated as the equilibrated thickness in saturated water vapor (>99 % relative humidity) divided by the thickness equilibrated in dry air (0 % relative humidity), measured by spectroscopic ellipsometry. For comparison, swelling ratios vs. film thickness are provided for TMC-MPD using the data series reported by Chan and Lee extrapolated to water activity 1.[27] The swelling ratio of TMC-BA is consistently 7 % to 10 %

higher than that of TMC-MPD with the same dry thickness. The TMC-BA membranes exhibit the same thickness-dependent swelling behavior as the TMC-MPD membranes, likely attributable to backfilling of the growing films via diffusion of fresh monomer into the membrane interior during the mLbL process, causing the membranes to not only become thicker but also more tightly cross-linked.

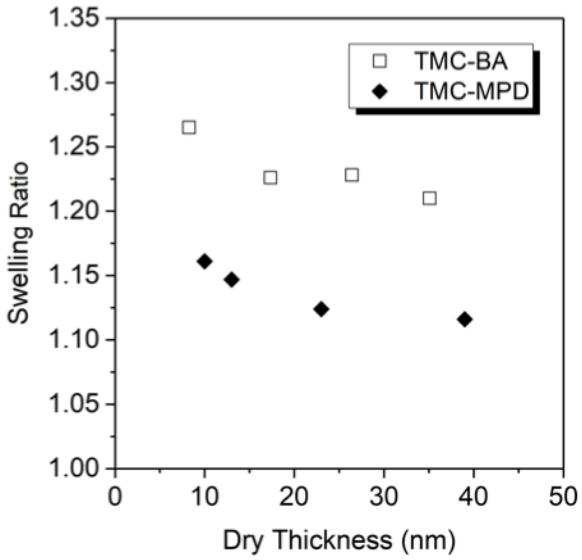


**Figure 3.** Swelling ratio of TMC-BA and TMC-MPD mLbL membranes in saturated water vapor vs. membrane dry thickness. In all cases the error bars are smaller than the symbols. The TMC-MPD series is reproduced from Chan and Lee, extrapolated to water activity 1.[27]

The thickness-dependent swelling of the mLbL membranes is paralleled by thickness-dependent transport behavior. The water permeance data shown in Figure 2 can be converted via eqn. 1 into the product of the water diffusion coefficient and the water sorption coefficient, $D_{w,m}$ $K_{w,m}$. The product of these two material parameters describes the combined effects of water

mobility and water partition in the membrane, and thus provides an intensive metric of water permeance. Similarly, the transport of salt can also be modeled using the solution-diffusion model. Here, owing to the large molar volume of the salt ions, the flux of salt, $J_s$, depends very weakly on pressure and can be well approximated by,[8]

$$J_s = \frac{D_{s,m}\, K_{s,m}}{h_m}\left(c_{s,f} - c_{s,p}\right) \tag{3}$$

The subscript *s* on the quantities in eqn. 3 denotes the NaCl salt, in contrast to the subscript *w* denoting water in eqn. 1. The feed NaCl concentration, $c_{s,f}$, is recalculated at each time of collection, based on the total volumes and concentrations of the collected permeate solution, $c_{s,p}$. Both derived data sets, $D_{w,m}\, K_{w,m}$ vs. film thickness and $D_{s,m}\, K_{s,m}$ vs. film thickness, as well as the ratio of the salt transport constants to the water transport constants, ($D_{s,m}\, K_{s,m}$) / ($D_{w,m}\, K_{w,m}$), are shown in Figure 4.

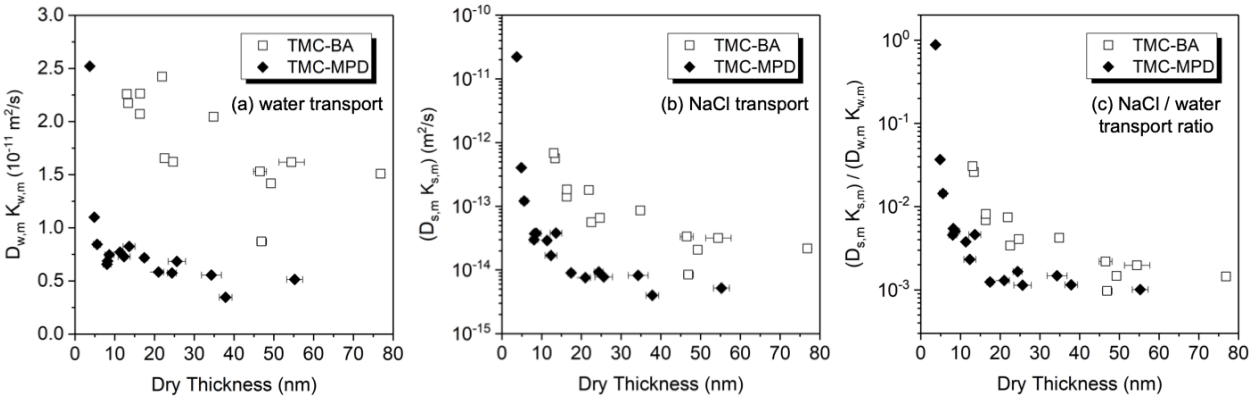


**Figure 4.** Products of the diffusion coefficient, *D*, and sorption coefficient, *K*, within a TMC-BA or TMC-MPD mLbL membrane vs. membrane dry thickness for (a) water, and (b) NaCl. The ratio of the NaCl transport constant product and the water transport constant product is also shown (c). The error bars represent one standard deviation of the data ($n$ = 3 to 5), which is taken

as the experimental uncertainty of the measurement. Some error bars are smaller than the symbols.

At all membrane thicknesses, TMC-BA exhibits higher water and salt partitioning and mobility than TMC-MPD. Furthermore, both membrane chemistries exhibit evolution of intensive transport properties with film thickness. For TMC-MPD, $D_{w,m}$ $K_{w,m}$ and $D_{s,m}$ $K_{s,m}$ stabilize above a critical film thickness, approximately 30 nm for water and 20 nm for salt. This trend suggests that the network initially becomes more tightly cross-linked with an increasing number of deposition cycles due to backfilling and reaction of residual functional groups in the membrane interior, until a saturated barrier layer forms at intermediate thicknesses and property evolution slows or stops. For TMC-BA, stabilization is more gradual, but the series converges to constant $D_{w,m}$ $K_{w,m}$ and $D_{s,m}$ $K_{s,m}$ values above approximately 50 nm. The lack of a sharp transition from a lightly cross-linked regime to a densely cross-linked regime likely reflects the inaccessibility of residual functional groups in the membrane interior, owing to poor reactivity or steric bulk of the BA monomer relative to MPD. If BA monomer cannot easily diffuse into the growing PA network but is restricted to reaction at the free surface, the film will continue to grow but will be slower to form a tightly cross-linked network. This observation is consistent with the tendency of IP TMC-BA membranes to exhibit very high water permeance per thickness but poor NaCl rejection; the severe kinetic limitations of this system require a stepwise process like mLbL, using good solvents that swell the network, to provide monomer accessibility to the interior in order to form any densely cross-linked material. An IP process is not conducive to dense network formation with the TMC-BA chemistry.

## Conclusion

In conclusion, mLbL deposition of TMC and BA enables the formation of tightly cross-linked network structures inaccessible by other synthesis methods, and a sufficiently dense network is necessary to facilitate exclusion of monovalent salts in RO. Using this mLbL approach, we have presented the first PA membranes based exclusively on the TMC-BA chemistry capable of greater than 90 % NaCl rejection. At the minimum thicknesses compatible with RO performance membranes composed of TMC-BA exhibit nearly 50 % higher water permeance than their TMC-MPD counterparts.

## ASSOCIATED CONTENT

### Supporting Information

The Supporting Information is available free of charge at…

Additional information regarding materials, membrane synthesis, membrane characterization, solubility of 3,5-diaminobenzoic acid in different organic solvents, growth rates of mLbL TMC-BA and TMC-MPD membranes, x-ray photoelectron spectra of TMC-BA and TMC-MPD showing carboxylic acid content, plots of water permeance vs. reciprocal membrane thickness, and measurement of water contact angle.

## AUTHOR INFORMATION

### Corresponding Author

Christopher M. Stafford – Materials Science and Engineering Division, National Institute of Standards and Technology, Gaithersburg, MD 20899, USA; orcid.org/0000-0002-9362-8707

Email: chris.stafford@nist.gov

## Authors

William D. Mulhearn - Materials Science and Engineering Division, National Institute of Standards and Technology, Gaithersburg, MD 20899, USA; orcid.org/ 0000-0001-6249-178X

Christopher M. Stafford – Materials Science and Engineering Division, National Institute of Standards and Technology, Gaithersburg, MD 20899, USA; orcid.org/0000-0002-9362-8707

## Author Contributions

The manuscript was written through contributions of all authors. All authors have given approval to the final version of the manuscript

## ACKNOWLEDGMENTS

W.D.M. acknowledges financial support from the National Research Council through the Research Associateship Program. Official contribution of the National Institute of Standards and Technology; not subject to copyright in the United States.

## References

(1) Elimelech, M.; Phillip, W. A. The Future of Seawater Desalination: Energy, Technology, and the Environment. *Science* **2011**, *333* (6043), 712–717. https://doi.org/10.1126/science.1200488.

(2) Geise, G. M.; Lee, H.-S.; Miller, D. J.; Freeman, B. D.; McGrath, J. E.; Paul, D. R. Water Purification by Membranes: The Role of Polymer Science. *J. Polym. Sci. B Polym. Phys.* **2010**, *48* (15), 1685–1718. https://doi.org/10.1002/polb.22037.

(3) Cadotte, J. E.; King, R. S.; Majerle, R. J.; Petersen, R. J. Interfacial Synthesis in the Preparation of Reverse Osmosis Membranes. *J. Macromol. Sci. Part A-Chem.* **1981**, *15* (5), 727–755. https://doi.org/10.1080/00222338108056764.

(4) Ghosh, A. K.; Jeong, B.-H.; Huang, X.; Hoek, E. M. V. Impacts of Reaction and Curing Conditions on Polyamide Composite Reverse Osmosis Membrane Properties. *J. Memb. Sci.* **2008**, *311* (1–2), 34–45. https://doi.org/10.1016/j.memsci.2007.11.038.

(5) Lee, K. P.; Arnot, T. C.; Mattia, D. A Review of Reverse Osmosis Membrane Materials for Desalination—Development to Date and Future Potential. *J. Memb. Sci.* **2011**, *370* (1–2), 1–22. https://doi.org/10.1016/j.memsci.2010.12.036.
(6) Lee, A.; Elam, J. W.; Darling, S. B. Membrane Materials for Water Purification: Design, Development, and Application. *Environ. Sci.: Water Res. Technol.* **2016**, *2* (1), 17–42. https://doi.org/10.1039/C5EW00159E.
(7) Klaysom, C.; Hermans, S.; Gahlaut, A.; Van Craenenbroeck, S.; Vankelecom, I. F. J. Polyamide/Polyacrylonitrile (PA/PAN) Thin Film Composite Osmosis Membranes: Film Optimization, Characterization and Performance Evaluation. *J. Memb. Sci.* **2013**, *445*, 25–33. https://doi.org/10.1016/j.memsci.2013.05.037.
(8) Wijmans, J. G.; Baker, R. W. The Solution-Diffusion Model: A Review. *J. Memb. Sci.* **1995**, *107* (1–2), 1–21. https://doi.org/10.1016/0376-7388(95)00102-I.
(9) Roh, I. J.; Park, S. Y.; Kim, J. J.; Kim, C. K. Effects of the Polyamide Molecular Structure on the Performance of Reverse Osmosis Membranes. *J. Polym. Sci. B: Polym. Phys.* **1998**, *36* (11), 1821–1830.
(10) Saha, N. K.; Joshi, S. V. Performance Evaluation of Thin Film Composite Polyamide Nanofiltration Membrane with Variation in Monomer Type. *Journal of Membrane Science* **2009**, *342* (1–2), 60–69. https://doi.org/10.1016/j.memsci.2009.06.025.
(11) Gupta, K. C. Synthesis and Evaluation of Aromatic Polyamide Membranes for Desalination in Reverse-osmosis Technique. *J. Appl. Polym. Sci.* **1997**, *66*, 643–653.
(12) Aiba, M.; Tokuyama, T.; Baba, S.; Matsumoto, H.; Tomioka, H.; Higashihara, T.; Ueda, M. Improvement in Semipermeable Membrane Performance of Wholly Aromatic Polyamide Through an Additive Processing Strategy. *J. Polym. Sci. Part A: Polym. Chem.* **2014**, *52* (9), 1275–1281. https://doi.org/10.1002/pola.27113.
(13) Ahmad, A. L.; Ooi, B. S.; Choudhury, J. P. Preparation and Characterization of Co-Polyamide Thin Film Composite Membrane from Piperazine and 3,5-Diaminobenzoic Acid. *Desalination* **2003**, *158*, 101–108.
(14) Ahmad, A. L.; Ooi, B. S.; Wahab Mohammad, A.; Choudhury, J. P. Development of a Highly Hydrophilic Nanofiltration Membrane for Desalination and Water Treatment. *Desalination* **2004**, *168*, 215–221. https://doi.org/10.1016/j.desal.2004.07.001.
(15) Ahmad, A. L.; Ooi, B. S.; Mohammad, A. W.; Choudhury, J. P. Composite Nanofiltration Polyamide Membrane: A Study on the Diamine Ratio and Its Performance Evaluation. *Ind. Eng. Chem. Res.* **2004**, *43* (25), 8074–8082. https://doi.org/10.1021/ie0497994.
(16) Kim, J.-J.; Kim, C.-K.; Kim, S.-Y. Composite Reverse Osmosis Membrane Having Active Layer of Aromatic Polyester or Copolymer of Aromatic Polyester and Aromatic Polyamide. 5,593,588, January 14, 1997.
(17) Karode, S. K.; Kulkarni, S. S.; Suresh, A. K.; Mashelkar, R. A. New Insights into Kinetics and Thermodynamics of Interfacial Polymerization. *Chemical Engineering Science* **1998**, *53* (15), 2649–2663. https://doi.org/10.1016/S0009-2509(98)00083-9.
(18) Ji, J.; Dickson, J. M.; Childs, R. F.; McCarry, B. E. Mathematical Model for the Formation of Thin-Film Composite Membranes by Interfacial Polymerization: Porous and Dense Films. *Macromolecules* **2000**, *33* (2), 624–633. https://doi.org/10.1021/ma991377w.
(19) Freger, V. Kinetics of Film Formation by Interfacial Polycondensation. *Langmuir* **2005**, *21* (5), 1884–1894. https://doi.org/10.1021/la048085v.

(20) Nadler, R.; Srebnik, S. Molecular Simulation of Polyamide Synthesis by Interfacial Polymerization. *Journal of Membrane Science* **2008**, *315* (1–2), 100–105. https://doi.org/10.1016/j.memsci.2008.02.023.
(21) Oizerovich-Honig, R.; Raim, V.; Srebnik, S. Simulation of Thin Film Membranes Formed by Interfacial Polymerization. *Langmuir* **2010**, *26* (1), 299–306. https://doi.org/10.1021/la9024684.
(22) Ukrainsky, B.; Ramon, G. Z. Temperature Measurement of the Reaction Zone during Polyamide Film Formation by Interfacial Polymerization. *Journal of Membrane Science* **2018**, *566*, 329–335. https://doi.org/10.1016/j.memsci.2018.09.011.
(23) Johnson, P. M.; Yoon, J.; Kelly, J. Y.; Howarter, J. A.; Stafford, C. M. Molecular Layer-by-Layer Deposition of Highly Crosslinked Polyamide Films. *J. Polym. Sci. B Polym. Phys.* **2012**, *50* (3), 168–173. https://doi.org/10.1002/polb.23002.
(24) Chan, E. P.; Lee, J.-H.; Chung, J. Y.; Stafford, C. M. An Automated Spin-Assisted Approach for Molecular Layer-by-Layer Assembly of Crosslinked Polymer Thin Films. *Review of Scientific Instruments* **2012**, *83* (11), 114102. https://doi.org/10.1063/1.4767289.
(25) Gu, J.-E.; Lee, S.; Stafford, C. M.; Lee, J. S.; Choi, W.; Kim, B.-Y.; Chan, E. P.; Chung, J. Y.; Bang, J.; Lee, J.-H. Molecular Layer-by-Layer Assembled Thin-Film Composite Membranes for Water Desalination. *Adv. Mater.* **2013**, *25*, 4778–4782.
(26) Gu, J.-E.; Lee, J. S.; Park, S.-H.; Kim, I. T.; Chan, E. P.; Kwon, Y.-N.; Lee, J.-H. Tailoring Interlayer Structure of Molecular Layer-by-Layer Assembled Polyamide Membranes for High Separation Performance. *Appl. Surf. Sci.* **2015**, *356*, 659–667. https://doi.org/10.1016/j.apsusc.2015.08.119.
(27) Chan, E. P.; Lee, S. C. Thickness-Dependent Swelling of Molecular Layer-by-Layer Polyamide Nanomembranes. *J. Polym. Sci. Part B: Polym. Phys.* **2017**, *55* (5), 412–417. https://doi.org/10.1002/polb.24285.